ACS APPLIED MATERIALS & INTERFACES

Research Article

www.acsami.org

Ultrasmooth Silver Thin Film on PEDOT:PSS Nucleation Layer for Extended Surface Plasmon Propagation

L. Ke,* S. C. Lai, H. Liu, C. K. N. Peh, B. Wang, and J. H. Teng*

Institute of Materials Research and Engineering, Agency for Science, Technology and Research (A*STAR), 3 Research Link, Singapore 117602

ABSTRACT: Poly(3,4-ethylene dioxythiophene):poly(styrene sulfonate) (PEDOT:PSS) layers are used as the nucleation (seed) layer to reduce surface roughness of the overlying silver (Ag). The technique leads to ultrasmooth Ag thin films with a minimum surface roughness of 0.8 nm. The mechanism contributing to the improvement is explained on the basis of better wetting of Ag on PEDOT:PSS, and properties of the nucleation layer on the aspects of surface energy, surface adhesive force, and surface morphology influencing Ag wetting and growth pattern are being discussed. The surface plasmon resonance (SPR) shows significant improvement, in terms of the Figure of Merits (FOM), as the surface roughness on Ag films is reduced. A lower light scattering and longer plasmon propagation of maximum 15.3 μm are also realized on a smoother Ag surface. The results indicate great potential on the application of combined PEDOT:PSS/Ag structure as an effective and economically feasible design solution for plasmonic and optical metamaterials devices.

KEYWORDS: *surface plasmon resonance, metamaterials, silver, PEDOT:PSS, surface roughness, propagation length*

I. INTRODUCTION

Polycrystalline silver (Ag) thin films are commonly developed by depositing the metallic particles directly on substrates using electron beam evaporation, chemical vapor depositio,n or sputtering. The resulting thin films usually possess surface roughness in the range of a few nanometers.[1,2] Such surface roughness is less than ideal for new-generation photonic devices, based on plasmonics or meta-materials. For advance applications such as superlens[3] and hyperlens,[4] Ag films with subnanometer surface roughness are vital for achieving low-loss surface plasmon propagation, as well as ultrahigh resolution subdiffraction and imaging. To satisfy such an unprecedented requirement on the surface qualities of Ag in plasmonic devices, researchers are intensifying their investigations in techniques to modify the film's growth mechanisms. Recent experiments on using nucleation (or seed growth) layer[5−7] to alter the growth mechanism of Ag thin films have succeeded in achieving ultrasmooth surfaces with subnanometer roughness and superior surface plasmon propagation (SPP).

Materials which have been used as the nucleation layer for fabricating ultrasmooth Ag films include germanium (Ge),[5−7] nickel (Ni),[6] and chromium (Cr).[8] The nucleation thin films are usually formed on the substrates via deposition techniques such as E-beam or thermal evaporation, thus creating an intermediate layer upon which the Ag thin films are being developed. The purpose of the nucleation layer is to increase the adhesion of Ag atoms on the substrate and bring about an improved interfacial wetting. Therefore, it is conceivable that the smoothness of the Ag film may be influenced by factors associated with the properties of its underlying nucleation film. These properties may include the surface tension,[9] surface adhesion, and surface morphology.[10]

The influence of the surface energies can be inferred from the Young−Dupré equation for the spreading coefficient (S).[9] Based on the relationship, nucleation materials with high surface tensions may facilitate wetting of the covering atoms. On the other hand, the property of surface adhesion can be associated with the existence of polar chemical groups in some nucleation materials. These polar groups can induce transient polarizations on the overlying thin film, and establish van der Waal's forces between atoms of the two layers at the interface. Such mutual attraction forces can contribute an improved interfacial wetting. Last but not least, the effect of the nucleation film's surface morphology can be explained with the wetting models provided by Wenzel and Cassie−Baxter.[10] As explained by the two models, the smoothness of the Ag films may respond differently with that of the underlying nucleation layer, depending on the wetting condition imposed by the latter.

Interfacial wetting also determines the growth mechanisms[11−15] of Ag typically described by the models of Volmer−Weber (VW)[11] and Stranski−Krastanov (SK).[12] In the Volmer−Weber model, atoms of the thin film tend to coalesce with each other under a stronger adatom−adatom cohesive force and a weaker surface adhesive force. This gives rise to three-dimensional (3D) islands nucleating on the substrate at the initial phase of the deposition process. On the other hand, the Stranski−Krastanov model describes the growth of the thin film to begin with a uniform layer-by-layer (LbL) nucleation pattern before transitioning to the 3D island growth mode. The initial LbL growth is attributed to a stronger surface adhesive force, which prevents the adatoms from coalescing. To develop ultrasmooth Ag film of nanoscale thickness, it is critical to shift the growth pattern toward the SK growth model, and this can be achieved by modifying the

Received: October 10, 2011
Accepted: February 16, 2012
Published: February 16, 2012

   dx.doi.org/10.1021/am201391f | ACS Appl. Mater. Interfaces 2012, 4, 1247−1253

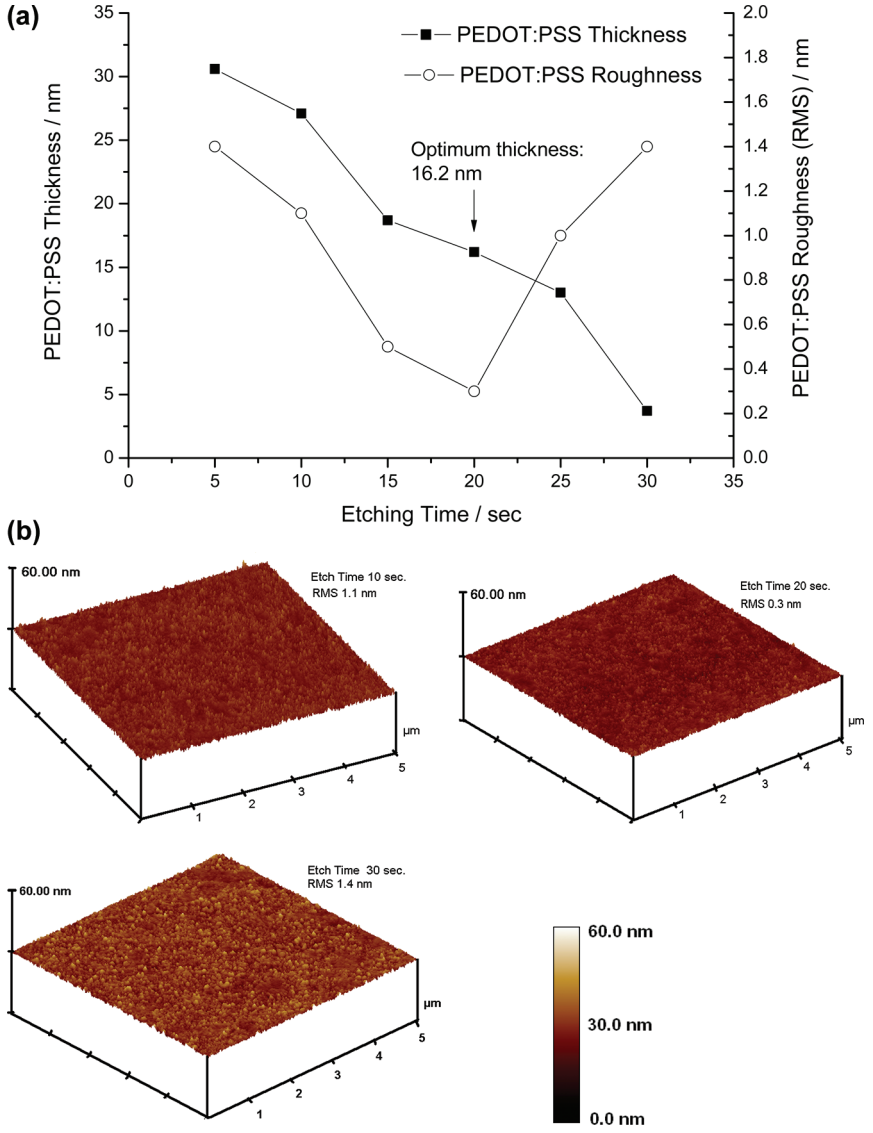

Figure 1. (a) Graphic showing that the PEDOT:PSS roughness is reduced as etching continued until 20 s; the surface roughness of the film reverted upon excessive etching beyond 20 s. (b) AFM images of the PEDOT:PSS surface at various stages of etching; the homogeneous tone of the image, corresponding to film with 20 s of etching, is indicative of a high level of smoothness, whereas spots with uneven tones that appeared on the film correspond to areas that were subjected to 30 s of etching, which suggested the formation of pinholes.

surface adhesive force of the substrate with the addition of a seed layer.

Consistent with the above perceptions on the role and influence of the nucleation layer, recent experiments have shown that Ag thin films can achieve a surface roughness of ~0.7 and 1.3 nm on Ge and Ni seed layer on quartz substrates, respectively.[6] With such an ultrasmooth morphology, the surface plasmon resonance (SPR) on the Ag film has since improved significantly in the Figure of Merits (FOMs). As reported by Liu et al.,[6] it was observed that the Ag film on Ni nucleation layer increased in the surface plasmon resonance (SPR) FOM by 35%, as compared to that of pure Ag on the substrate. However, the SPR properties are also influenced by the adsorptive damping effects[16,17] of the underlying nucleation layer, as epitomized in the case of Ge. In the same work by Liu et al.,[6] the improved surface morphology of Ag film on Ge seed layer may not be even sufficient to compensate for the loss of SPR at the excitation wavelength of 630 nm. The paper ascribed the loss to the damping effects associated with the inherent dielectric properties of the seed materials. Therefore, to achieve excellent SPR and extended propagation length, the nucleation layer must not only provide good interfacial wetting on Ag, but also minimal SPR quenching known to some metalloids.

Therefore, it is interesting to explore the use of polymers as an alternative nucleation material for the fabrication of ultrasmooth Ag films with high-quality SPR. Polymers can provide improved interfacial wetting on the surfaces of the quartz (or glass) substrates and Ag films. The improved wetting is realized on the basis that organic−metal bonding can be stronger than the metal−metal or metal−metalloid bonding provided by Ge or Ni seed layers. Furthermore, polymers can impose less SPR damping effects attributable to the dielectrics in the excitation wavelength of interests, therefore leading to a higher FOM for SPR and longer surface plasmon propagation.

In this work, we are examining the use of poly(3,4-ethylene dioxythiophene):poly(styrene sulfonate) (PEDOT:PSS) as the nucleation layer for fabricating ultrasmooth Ag film. PE-

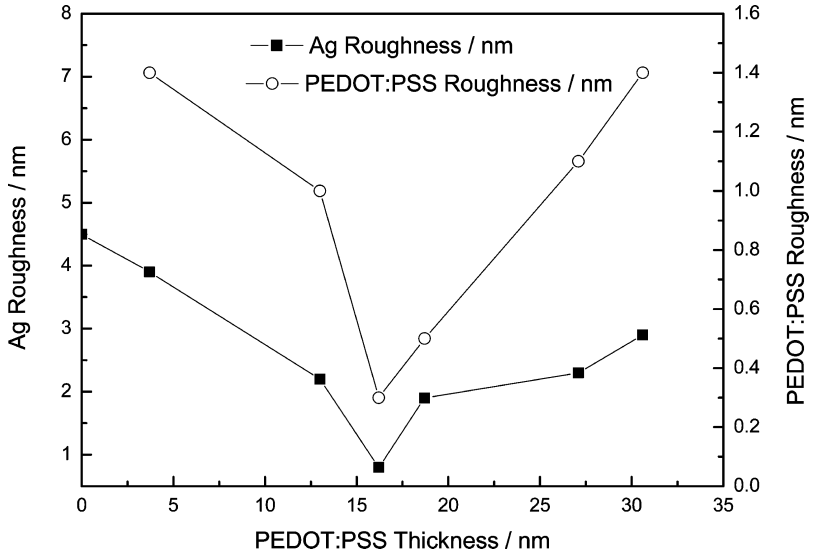

Figure 2. Surface roughness of Ag films correlates strongly with that of the underlying PEDOT:PSS films.

DOT:PSS possesses high optical transparency, good conductivity for holes, and a relatively high work function, and it has been widely used as the buffer layer in organic light-emitting diodes (OLEDs).[18] PEDOT:PSS can also turn out to be a promising candidate to serve as the seed material for Ag films in plasmonic devices, because of its inherently low dielectric constant in magnitude, relative to Ag (typically 9.7). The low dielectric constant of PEDOT:PSS facilitates SP coupling at the Ag/PEDOT:PSS interface, and enhances the FOM of SPR.[19] On the other hand, known seed materials such as Ge and Ni possess a dielectric constant nearer to that of Ag, and this can be disadvantageous to SP coupling at the interface. A quick simulation of SPR reflectivity curves based on PEDOT:PSS, Ge and Ni would indicate that PEDOT:PSS should give rise to better SPR, with respect to Ge and Ni.

Currently, however, the role of PEDOT as the nucleation layer and its effects on the surface morphology and plasmon resonance of the overlying Ag thin films has not been adequately addressed. This is an area that warrants further in-depth studies before the polymer can be practically applied for plasmon enhancement in the future generation of photonic devices.

II. EXPERIMENTS

Preparing Samples of Variable PEDOT:PSS on Fixed Ag Thicknesses (Sample Batch 1). Quartz substrates (C-grade) with dimensions of 15 mm × 15 mm × 0.4 mm (H) and a refractive index of 1.46 were dry-cleaned in a reactive ion etch (RIE) chamber. The substrates were treated with oxygen plasma set at a flow rate of 30 ppm. The substrates then were examined via atomic force microscopy (AFM), and the surface roughness was noted to be 0.1 nm. PEDOT:PSS solution was then spin-coated onto the substrates at 2000 rpm to achieve an initial thickness of ∼30 nm and subsequently etched down via RIE. The time of etching varied from 5 s to 25 s, by intervals of 5 s, to yield PEDOT:PSS layers of different thickness. Reflowing was done at 150 °C for 5 min to achieve a smoother surface. A 50-nm-thick Ag film was subsequently deposited under vacuum at room temperature, using an Edwards Model Auto306 Electron-beam evaporator at a base pressure of ∼5×10^{-7} mTorr; the deposition rate is 5 Å/s. A pure Ag film ∼50 nm thick, without PEDOT:PSS, on a quartz substrate was also fabricated, for the sake of comparison.

Preparing Samples of Variable Ag and Fixed PEDOT:PSS Thickness (Sample Batch 2). Quartz substrates with the same dimensions and refractive index as that previously described were dry-cleaned in an RIE chamber under the same condition. PEDOT:PSS solution was then spin-coated onto the substrates at 2000 rpm to achieve an initial thickness of ∼30 nm and subsequently etched down via RIE for 15 s to yield a thickness of ∼20 nm. Reflowing was again done at 150 °C for 5 min to achieve a smoother surface. Ag films over the thickness range of 5−50 nm over the interval of ∼5 nm were subsequently deposited on the substrate under vacuum, using an Edwards Model Auto306 Electron-beam evaporator at a base pressure of ∼5×10^{-7} mTorr. Another batch of Ag films of the same thicknesses were also deposited directly (without any nucleation layer) on similarly cleaned quartz substrates under the same set of conditions to act as references. The deposition rate is the same of 5 Å/s at room temperature.

Measuring Film Surface Roughness, Thickness, and SPR. The surface morphology and root-mean-square (rms) surface roughness of the Ag films were then characterized using a multimode atomic force microscopy (AFM) system from Digital Instruments, configured to tapping mode. The samples were scanned over an area of 5 μm^2 at a tip velocity of 2 μm/min with a corresponding scan rate of 1 Hz.

The film thickness was characterized by variable-angle spectroscopic ellipsometry (WVASE32 software, J.A. Woollam Co.). The data were acquired by scanning over an angle range of 65°−75°, in steps of 5°, over the spectral range of 300−800 nm, in steps of 2 nm.

SPR spectroscopy was conducted in the Kretschmann−Raether[20,21] configuration, using a BK7 prism and a linear polarized He−Ne laser light (λ = 632.8 nm, power of 20 mW), assisted by a matching index oil with a refractive index of 1.55. The light scattering and other information relevant to propagation length of the surface plasmons (SPs) on the Ag/PEDOT:PSS film were captured through a microscope and a black/white charge-coupled device (CCD) camera. To avoid saturation of the CCD camera, the light intensity was adjusted by a neutral density filter and the power was attenuated to ∼3 mW. The obtained digitized two-dimensional (2D) image reflected the distribution of the intensity of scattered light over the surface. By calculating the distribution of the intensity of the scattered light, the attenuated propagation length can be obtained using the analytical model, taking the roughness into consideration.

III. RESULTS AND ANALYSIS

Effects of Etching on PEDOT:PSS Thickness and Surface Roughness. The PEDOT:PSS layers etched to different thicknesses via RIE were examined using AFM, and the graph of the surface roughness and thickness versus etching time is plotted in Figure 1a. It was observed that, as the

PEDOT:PSS layers were etched over a longer duration, the reduction of thickness was generally accompanied by a reduction in the surface roughness prior to 20 s of etching. Further etching beyond 20 s, however, increased the surface roughness of the polymer layer. The initial improvement in the surface roughness was likely due to the smoothening effect of prolonged etching, which eliminates any subnanometer unevenness in the amorphous morphology of the polymer. However, excessive etching resulted in overly thin and discontinuous films on the substrate, hence increasing the surface roughness. Further examination on the AFM images on PEDOT:PSS surface revealed islands of pinholes, which began to appear and proliferate after 20 s of etching. The results indicated that, while prolonged etching could have effectively smoothen the surface of the polymer, roughness could also return significantly when excessive etching led to discontinuous films.

Effects of PEDOT:PSS on Ag Surface Roughness. In the samples fabricated under "Batch 1", the surface roughness of the Ag films deposited on the PEDOT:PSS layer of various thicknesses was measured via AFM. The Ag roughness measurements were then compared to that of the PEDOT:PSS surface characterized above, as plotted in Figure 2. It could be observed that the roughness measurements of the Ag and PEDOT:PSS were highly correlated with each other. Consistent with the roughness of the PEDOT:PSS, the Ag surface became smoother as the PEDOT:PSS films were etched thinner. This trend continued until the PEDOT:PSS thickness reached 16.2 nm, which was produced at 20 s of etching. As the polymer films became thinner upon further etching, the roughness of the Ag surface began to increase, along with that of the underlying PEDOT:PSS, because of the formation of pinholes on the nucleation layer, as a result of excessive etching.

The above observation demonstrated that the PEDOT:PSS nucleation layer had effectively improved the surface morphology of the overlying Ag thin film. In the absence of the polymer layer, the surface roughness of the Ag film on pure quartz surface exhibited the highest values of 4.5 nm. With the insertion of the nucleation film, an improved wetting surface was created which, in turn, resulted in a more homogeneous growth of the Ag film. The effect led to the realization of an ultrasmooth Ag film achieving the minimum roughness of 0.8 nm on the PEDOT:PSS layer with a thickness of 16.2 nm and roughness of 0.3 nm. This roughness on the Ag film surface was comparable to the reported values of Ag thin films developed on other types of nucleation materials, such as Ge.[5,6]

The improvement in the wetting was likely due to the increase in the surface adhesive forces exhibited on the nucleation surface, which was made of a polar material comprising of positively charged conjugated PEDOT polymer, and a negatively charged deprotonated sulfonyl group. Such a polar property was capable of inducing weak polarization on the interfacial Ag atom, so that a weak interactive force (van der Waal's force) was established to attract the surface atom of Ag toward the nucleation surface.

It was noted that the PEDOT:PSS solution possessed a relatively low surface energy (typically 71 mJ m^{-2} (from ref 18)), compared to that of SiO_2 (typically 260 mJ m^{-2} (from ref 7)), which allows the nucleation layer to form a good wetting on the quartz substrate. However, the polymer was perceived to possess a much higher surface energy in its solid phase, in view of the strong interlocking covalent bonding formed between the polymer subunits. Such a strong intermolecular bonding within the polymer could present a relatively high surface energy, compared to that of a metal with large atomic radius such as Ag in its metastable phase at the point of deposition. Therefore, it was conceivable that the effects of the relative surface tension between the Ag film and the nucleation layer also contributed to the improvement in the wetting, as expounded by the Young–Dupré equation.[9]

Interestingly, it was observed that the Ag film and underlying PEDOT:PSS tended to be related to each other more closely by the Cassie–Baxter[10] model rather than that of Wenzel,[10] so that surface roughness of the Ag film increases with that of PEDOT:PSS. The reason could be ascribed to incomplete wetting of Ag on the nucleation layer, so that it did not fill up the nanometer-scale grooves on the surface, despite the improvement in interfacial wettability. This was substantiated on the basis that Ag typically possessed a considerable surface energy of 1.2–1.4 J m^{-2}.[7] Incomplete wetting gave rise to a lower f parameter in the Cassie's law equation (that is, the fraction of solid surface actually in contact with the Ag), and this led to an increase in the contact angle. Another possible cause of incomplete wetting, albeit to a lesser extent, was the presence of remnant air pockets trapped in the roughness groove on the PEDOT:PSS surface, not withstanding that the deposition was performed under vacuum conditions.

Effects of PEDOT:PSS on Ag Growth Mechanism. Previously, it had been observed that Ag tended to adopt growth patterns typical of Volmer–Weber model on crystalline or polycrystalline semiconductor substrates, such as Si[15] or GaAs.[11,14] Some of the reports[11,14,15] had shown that Ag islands began to coalesce as soon as the metal particles were being deposited on the substrates. The mechanism of island formation was facilitated by the strong adatom–adatom forces in Ag, as reflected by its high surface energy. However, the nucleation layer can modify the growth behavior by providing a surface of either high tension or high adhesion, to bring about an improvement in the interfacial wettability.

To investigate the influence of the nucleation layer on the Ag growth mechanism, samples fabricated under "Batch 2" (Ag films of variable thicknesses deposited on a fixed, 20-nm-thick PEDOT:PSS) were measured on the surface roughness. The reference samples, which were comprised of Ag films with the same thicknesses deposited directly on quartz substrates, were also subjected to surface roughness measurement, for the purpose of comparison. The transition of the surface roughness, as plotted in Figure 3, would reflect the disappearance or formation of Ag islands during the course of the deposition.

The measurements showed that the reference samples, in the absence of the nucleation layer, assumed a higher surface roughness (of ~4 nm) at the start of the deposition. The high surface roughness at the initial suggested that the Ag islands had already formed at the onset of deposition. In addition, in the reference samples, the surface roughness increased with the deposition as more Ag became available to coalesce into the 3D islands, under the effect of strong adatom–adatom interaction. The behavior, as epitomized by the Volmer–Weber model of growth, continued until a critical thickness of Ag (~30 nm) was deposited. Beyond this critical thickness, however, the surface roughness reduced rapidly, because the Ag islands began to grow and merge with each other under the influence of strong adatom–adatom interaction. Eventually, all the islands combined to produce a smoother surface on the thin film.

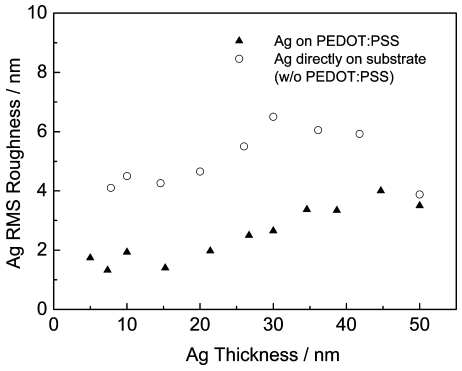

Figure 3. Transition of Ag films surface roughness in the course of deposition with and without the influence of the PEDOT:PSS nucleation layer.

On the other hand, Ag films on the PEDOT:PSS layer exhibited a much smoother surface, not exceeding 2 nm at the onset of deposition. As more Ag was deposited, the surface roughness increased very gradually, which was possibly due to the formation of Ag islands as the influence from the nucleation surface began to diminish. This pattern was consistent with the Stranski–Krastanov growth model, which suggested that the Ag films would adopt a LbL growth on a good wetting surface until attaining a certain critical thickness, before transitioning to the 3D island growth mode. It was worth highlighting that, generally, Ag films deposited on the PEDOT:PSS layer possessed a much smoother surface than the reference counterparts. This was strong evidence of improved surface wetting, which allowed the deposited Ag atoms to grow more homogeneously via a LbL pattern.

Ag Surface Plasmon Resonance (SPR) Properties. The surface plasmon resonance (SPR) of the Ag films deposited on PEDOT:PSS layers of different thicknesses ("Batch 1") were acquired in the plot of reflectance versus incident angle, as shown in Figure 4a. It could be observed that the reflectance intensity of the Ag film decreased as the PEDOT:PSS thicknesses were reduced, in accordance with the simulated results of Figure 4b. It was interesting to note that the experimental SPR exhibited a slight shift in the resonance angle. In the simulated results, where the effect of the surface roughness was excluded, the resonance angle was consistent for all PEDOT thicknesses. Therefore, the slight displacement of the resonance angle can be attributed to the surface roughness of the Ag films, or to the change in Ag grain size under the effects of different PEDOT:PSS layers.

The most important parameter that characterizes the SPR quality of a material is known as the Figure of Merit (FOM). The FOM of the SPR exhibited by the Ag films on different thickness of PEDOT:PSS was computed based on eq 1 and is plotted in Figure 5.

$$\mathrm{FOM} = \frac{\Delta R}{R_c} \times \frac{1}{\mathrm{FWHM}} \tag{1}$$

where ΔR is the difference of reflectivity between the critical angle and resonance angle, and R_c is the reflectivity at the critical angle.[22]

It was observed that the FOM increased on a smoother Ag surface enhanced by the PEDOT:PSS nucleation layer. In the absence of the nucleation layer, both the SPR FOM and Ag roughness exhibited the lowest and highest values, respectively. The SPR FOM increased as the Ag surface morphology was

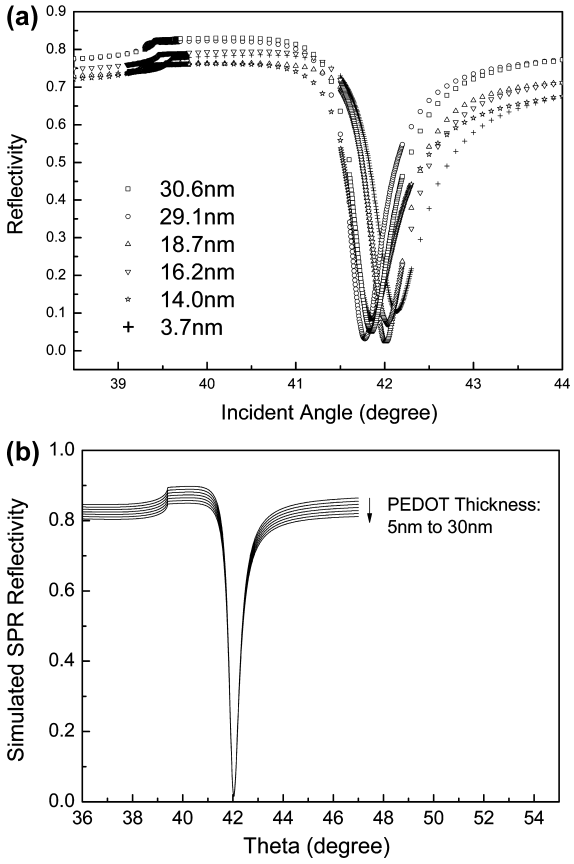

Figure 4. (a) Surface plasmon characteristics of the Ag films with the underlying PEDOT:PSS layers of different thickness; the resonance angle exhibited a slight displacement, because of the differing surface roughness of the films. (b) Simulated surface plasmon characteristics of the Ag films with the underlying PEDOT:PSS layers of different thickness; the resonance angle exhibited the same resonance angle when the effect of the surface roughness was excluded.

smoothened by the wetting effect of the PEDOT:PSS layer, and the optimum values on the sample were attained when the Ag film possessed the minimum roughness of 0.8 on a PEDOT:PSS layer 16.2 nm thick. The highest FOM of 2.87 was achieved in the experiment, which was a significant improvement over the reported values of 2.37 and 1.86 for Ag on Ni and Ge, respectively.[6] Compared to the SPR FOM of protected Ag thin film on Ti in the recent work of Touahir et al.[25] and Szunerits et al.,[26] our achieved value indicated a much higher quality. The results highlighted that the PEDOT:PSS nucleation layer had effectively enhanced the quality of SPR by providing an ultrasmooth optical surface without inducing SPR damping in our wavelength of interest.

Light Scattering and Surface Plasmon Propagation Length. The light scattering of the Ag films from "Batch 1" were studied, and the scattering profiles on the Ag surface with roughnesses of 0.8 and 3.9 nm are plotted in Figure 6. It was observed that the light spot was much more focused (as shown by a smaller diameter) on the smoother Ag film, compared to that on the rougher surface. With less scattering, the smoother Ag film enhanced by the PEDOT:PSS nucleation layer would result in a longer surface plasmon propagation (SPP) length.

dx.doi.org/10.1021/am201391f | ACS Appl. Mater. Interfaces 2012, 4, 1247–1253

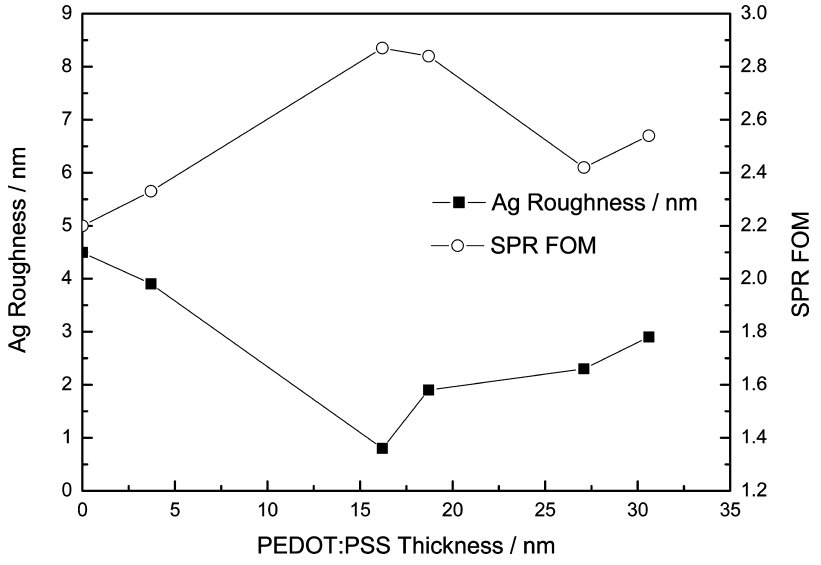

Figure 5. Graphics showing that the surface plasmon resonance (SPR) Figure of Merit (FOM) of the Ag films increases with the reduction of the surface roughness. FOM reached a maximum at a PEDOT:PSS thickness of 16.2 nm, where the Ag film achieved the minimum roughness.

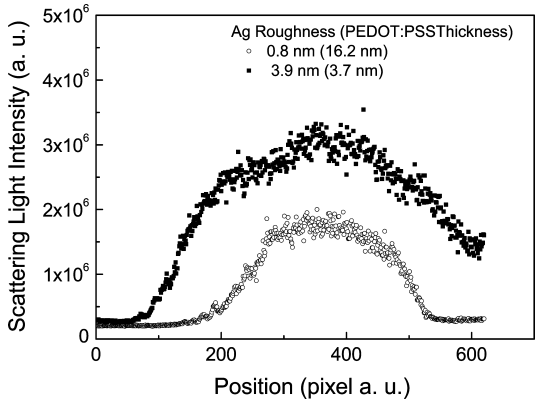

Figure 6. Light scattering profile of Ag films with surface roughnesses of 0.8 and 3.9 nm on the PEDOT:PSS layer. Ag film with the smoother surface exhibited a more-focused light spot than that with a rougher surface.

The SPP length could then be derived by curve-fitting the light scattering profile with eq 2 on the observed light density (F) along the surface:

$$F(x) \propto \exp\left(-\frac{x^2}{a^2}\right)\int_0^{\infty} \exp\left[-\frac{{x_1}^2}{a^2} \pm x_1\left(\frac{2x}{a^2}+\frac{1}{L_{sp}}\right)\right]dx_1 \quad (2)$$

where L_{sp} is the propagation length, a the geometrical width of the light spot, and the signs ($\pm$) correspond to the SPs propagating in the directions $x \rightarrow \mp\infty$.[23] The fitting and derivation are done using the Matlab program.

The above model was based on the equation of the Gaussian distribution describing the intensity of the irradiative spot focused by the laser beam on the surface, but simplified to assume one-dimensional (1D) propagation. The intensity along the propagation direction was taken to be proportional to the integral of the contributions from different cross sections of the irradiative spot while factoring the effects of surface plasmon attenuation along the propagation distance. In the model, it was also assumed that the surface roughness and light scattering were uniform over the propagation surface.

The computed SPP lengths of the samples are plotted in Figure 7, and it was observed that the propagation length

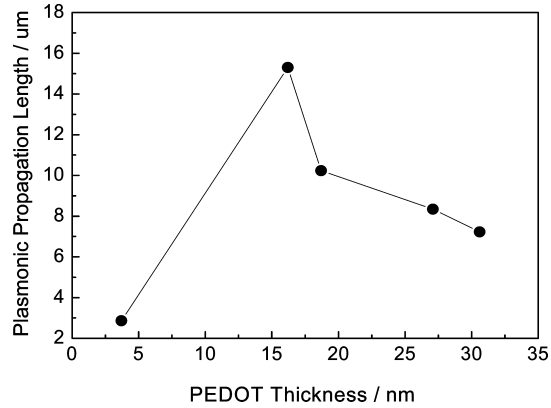

Figure 7. Graphic showing that the surface plasmon propagation (SPP) length peaked at the sample with a PEDOT:PSS layer 16.2 nm thick, upon which the Ag film exhibited the smoothest surface. The propagation length showed a strong correlation with the Ag surface smoothness.

increased as Ag surface roughness decreased. The improvement in the propagation length on a smoother Ag film could be explained by the above modeling equation (eq 2), which implied that a reduction in light scattering on a smoother surface would minimize propagation losses. Reflecting on the data in this experiment, the longest propagation of 15.3 μm was achieved on the Ag film developed on 16.2-nm-thick PEDOT:PSS film. This sample correspondingly provided the Ag film with the minimum surface roughness. The propagation length achieved at this juncture was a significant improvement over the propagation length of 2.4 μm for the Ag thin film reported earlier by Thost et al.,[24] and was also comparable to

the value of 18.8 μm for Ag on the Ni nucleation layer reported by Liu et al.[6]

IV. CONCLUSION

This paper has demonstrated that ultrasmooth Ag films could be achieved on a poly(3,4-ethylene dioxythiophene):poly-(styrene sulfonate) (PEDOT:PSS) nucleation layer on quartz substrates. Such surface roughness in subnanometer scale on Ag was realized on the basis of improved interfacial wetting provided on the nucleation surface. The improvement in the wetting was, in turn, mainly ascribed to the additional adhesive force and high surface energy presented by the polar PEDOT:PSS film.

The experiment had given rise to an interesting observation that the surface roughness of the Ag films and that of the nucleation films beneath assumed a direct relationship akin to the Cassie–Baxter Law. This indicates the importance of achieving an ultrasmooth morphology on the nucleation surface first, before high-quality Ag films of subnanometer roughness could be developed on them. The observation, in turn, highlighted the advantage of using PEDOT:PSS as the seed materials, in view that the polymer in solution could establish complete wetting on many substrates to produce an ultra-smooth film (as evident in the experiment), because of its relatively low surface tension.

The results had also provided an insight into how the nucleation layer had shifted the growth mechanism of Ag from the Volmer–Weber (VW) growth mode to that of Stranski–Krastanov (SK). The ability to shift the Ag growth pattern to follow the SK model has great significance, because it implies that an ultrasmooth surface can also be achieved on an ultrathin Ag layer when adatom–adatom nucleation is inhibited at the onset of the deposition.

With the surface roughness of the Ag film minimized to subnanometer scale, the quality on the surface plasmon resonance (SPR), in terms of the Figure of Merit (FOM), was greatly enhanced. There was no observable evidence of SPR quenching for the wavelength performed in the experiment. The light scattering characterization indicated that an ultrasmooth Ag surface could significantly reduce surface plasmon losses and effectively extend the surface plasmon propagation (SPP).

AUTHOR INFORMATION

Corresponding Author

*E-mail addresses: Karen-kl@imre.a-star.edu.sg (L.K.), jh-teng@imre.a-star.edu.sg (J.H.T.).

Notes

The authors declare no competing financial interest.

REFERENCES

(1) Kundu, S.; Hazra, S.; Banerjee, S.; Sanyal, M. K.; Mandal, S. K.; Chaudhuri, S.; Pal, A. K. *J. Phys. D: Appl. Phys.* **1988**, *31*, L73.
(2) Chi, Y.; Lay, E.; Chou, T. Y.; Song, Y. H.; Carty, A. *Chem. Vap. Deposition* **2005**, *11*, 206.
(3) Fang, N.; Lee, H.; Sun, C.; Zhang, X. *Science* **2005**, *308*, 534.
(4) Liu, Z. W.; Lee, H.; Xiong, Y.; Sun, C.; Zhang, X. *Science* **2007**, *315*, 1686.
(5) Logeeswaran, V. J.; Nobuhiko, P.; Kobayashi, M.; Saif, I.; Wu, W.; Chaturvedi, P.; Fang, X. N.; Wang, S. Y.; William, R. S. *Nano Lett.* **2009**, *9*, 178.
(6) Liu, H.; Wang, B.; Leong, E. S. P.; Yang, P.; Zong, Y.; Si, G. Y.; Teng, J. H.; Maier, S. A. *ACS Nano* **2010**, *4*, 3139.
(7) Chen, W. Q.; Thoreson, M. D.; Ishi, S.; Kildishev, A. V.; Shalaev, V. A. *Opt. Express* **2010**, *18*, 5124.
(8) Melpignano, P.; Cioarec, C.; Clergereaux, R.; Gherardi, N.; Villeneuve, C.; Datas, L. *Org. Electron.* **2010**, *11*, 1111.
(9) Geoghegan, M.; Krausch, G. *Prog. Polym. Sci.* **2003**, *28*, 261.
(10) Swain, P. S.; Lipowsky, R. *Langmuir* **1998**, *14*, 6772.
(11) Placidi, E.; Fanfoni, M.; Arciprete, F.; Patella, F.; Motta, N.; Balzarotti, A. *Mater. Sci. Eng., B* **2000**, *B69–70*, 243.
(12) Corcoran, S. G.; Chakarova, G. S.; Sieradzki, K. *Phys. Rev. Lett.* **1993**, *71*, 1585.
(13) Venables, J. A.; Spiller, G. D. T.; Hanbucken, M. *Rep. Prog. Phys.* **1984**, *47*, 399.
(14) Fanfoni, M.; Arciprete, F.; Patella, F.; Boselli, A.; Sgarlata, A.; Motta, N.; Balzarotti, A. *Surf. Sci.* **1998**, *419*, 24.
(15) Hanbücken, M.; Neddermeyer, H. *Surf. Sci.* **1982**, *114*, 563.
(16) Fontana, E. *Appl. Opt.* **2006**, *45*, 7632.
(17) Lee, H. I. *Opt. Commun.* **2009**, *282*, 2270.
(18) Cioarec, C.; Melpignano, P.; Gherardi, N.; Clergereaux, R.; Villeneuve, C. *Langmuir* **2011**, *27*, 3611.
(19) Hong, K. H.; Lee, J. L. *Electron. Mater. Lett.* **2001**, *7*, 77.
(20) Homola, J. R. *Sens. Actuators, B* **1999**, *54*, 3.
(21) Kurihara, K.; Nakamura, K.; Suzuki, K. *Sens. Actuators, B* **2002**, *86*, 49.
(22) Tsuda, Y.; Omoto, H.; Tanaka, K.; Ohsaki, H. *Thin Solid Films* **2006**, *502*, 223.
(23) Kolomenskii, A.; Noel, J.; Peng, S. Y.; Schuessler, H. *Appl. Opt.* **2009**, *48*, 5683.
(24) Thost, J. P.; Krieger, W.; Kroo, N.; Szentirmay, Z.; Walther, H. *Opt. Commun.* **1993**, *103*, 194.
(25) Touahir, L.; Niedziolka, J. J.; Galopin, E.; Boukherroub, R.; Gouget, L. A. C.; Solomon, I.; Petukhov, M.; Chazalviel, J. N.; Ozanam, F.; Szunerits, S. *Langmuir* **2010**, *26*, 6058.
(26) Szunerits, S.; Castel, X.; Boukherroub, R. *J. Phys. Chem. C* **2008**, *112*, 15813.